The International Journal of Advanced Manufacturing Technology (2020) 111:2589–2599
https://doi.org/10.1007/s00170-020-06188-8

ORIGINAL ARTICLE

Investigation of surface roughness in face milling processes

Muhammad Huzaifa Raza [1] · Faisal Hafeez [2] · Ray Y. Zhong [1] · Asif Imran [2]

Received: 19 August 2020 / Accepted: 28 September 2020 / Published online: 31 October 2020

Abstract
This study aims to investigate the effects of dry, minimum quantity lubrication (MQL), and nanofluid cutting conditions on surface roughness (Ra) and material removal rate (MRR) for Al6082-T6. Three controllable factors, namely, feed rate (Fr), spindle speed (Vs), and depth of cut (Dc) are studied at three levels using Taguchi method. Single-response optimization is conducted using S/N ratio and contour plots. Empirical models of Ra and MRR for all cutting conditions are developed, and analysis of variance (ANOVA) is used to measure the adequacy of these models. Experimental results reveal that 26~30% improvement in Ra could be observed when experimental setup shifted from dry to MQL, and 13~16% improvement is recorded when further shifted to nanofluid cutting condition. No remarkable effect of cutting conditions (dry, MQL, and nanofluid) is observed on MRR. Additionally, Vs is observed insignificant for MRR in all cutting conditions. The appropriate cutting conditions and optimum values of input variables are proposed to the practitioners for industrial machining and production when contemplating face milling processes.

Keywords Minimum quantity lubrication (MQL) · Nanofluid · Surface roughness · Face milling · Material removal rate (MRR)

Nomenclature

ANOVA	Analysis of variance
MQL	Minimum quantity lubrication
MRR	Material removal rate
Ra	Surface roughness
S/N ratio	Signal-to-noise ratio
Fr	Feed rate
Vs	Spindle speed
Dc	Depth of cut

1 Introduction

Face milling is the secondary process used for the cutting and finishing of parts. The process is employed for the fabrication of tooling for other processes with high accuracy in a suitable processing time [1] and also used in the parts of aerospace and automotive industries, where quality is the prime factor [2]. Surface roughness is the measure of quality in machined parts, highly depends upon controlling parameters: Fr, cutting speed, and Dc [3]. There is a need to optimize these controlling parameters to enhance the quality of parts as Ra is sensitive to Fr [4, 5]. It was observed that the parameters other than feed (axial and radial Dc and cutting speed) are also significant factors that affect the Ra [6]. Material removal rate is the second major measure, which need to be maximized without compromising the surface quality of the part [7]. The factors that contribute in achieving maximum MRR are Fr and Dc [8]. High Fr results in higher MRR but it also increase the cutting temperature which reduces the tool life [9] and surface quality [10]. Beside input parameters, cutting fluid has the prime importance in metal cutting processes for enhancing the quality of the workpiece by lubricating the tool. Workpiece interface lubrications (cutting fluid) improve the machining characteristics and workpiece's surface quality [11]. But flooded cooling increases the manufacturing cost by 16% [12]. To minimize the coolant cost, MQL technique was introduced. Researchers focused on MQL technique as it reduces the consumption of lubricant by sprinkling the blend of air and lubricant and as environmental friendly [13]. In MQL, coolant mixed with compressed air is sprayed at the tool-workpiece interface at a low flow rate [14]. It is reported that the MQL reduces the coolant consumption 3 times than flooded cooling

✉ Muhammad Huzaifa Raza
huzaifa@connect.hku.hk

[1] Department of Industrial and Manufacturing System Engineering, The University of Hong Kong, Pok Fu Lam, Hong Kong

[2] Department of Industrial Engineering, University of Engineering and Technology Taxila, Taxila, Pakistan

using flow rate 50–500 ml/h approximately. It is investigated that MQL produces superior surface finish than other conventional methods of lubrication [15, 16]. MQL not only improves the surface finish but also reduces cutting temperature and enhances the tool life by reducing the flank wear [17, 18] as it provides excess amount of oxygen at tool-workpiece interface forming the protective oxide layer [19]. But for material removal rate, it is evident that MQL did not show significant improvement for medium carbon steel [20].

To enhance the efficiency of MQL, nanoparticles are contaminated in the fluid. The addition of nanoparticles improves the surface quality [21]. It is claimed that 46% reduction in surface roughness was achieved as compared with the commonly used lubricant [12]. In nanofluid, particles form a lubrication film and fill the surface cavities which polish the surface and improve the surface quality [22, 23]. It is noticed that nanofluid exhibits better Ra as compared with base fluid [24]. However, increasing of nanoparticles concentration results in reduced Ra since the excess nanoparticles concentration enhances the viscosity of cutting fluid and fills the surface pores. Incoming nanoparticles shear off the existing ones and other ploughed off particles remain stuck on exfoliated film in tool-workpiece interface. Therefore, increased nanoparticles concentration may negatively influence the surface quality [25]. But the percentage improvement is different for soft and hard material while using MQL and nanofluid. And there is a need to study the trends of the input variables/parameters in different cutting conditions.

Number of statistical and mathematical techniques including response surface methodology, factorial design, Taguchi method, genetic algorithm, fuzzy logic, and artificial neural network have been used [26–32]. Among these techniques, genetic algorithm, fuzzy logic, and artificial neural network are the soft computing, while response surface methodology, factorial design, and Taguchi method are statistical techniques. Soft computing techniques also have the ability to predict the response measures, and repetitive hit and trial is used for prediction. However, statistical techniques require less number of experiments for the prediction and optimization. Therefore, Taguchi method has been observed with less number of experiments and also considered as cost-effective [33]. After the selection of suitable experimental design, various analysis techniques including multi-criteria decision-making (MCDM) analysis, grey relational analysis (GRA), and analysis of variance (ANOVA) have also been used by the researchers in order to optimize the response measures [34–36].

Industrial sector is still in efforts to obtain a proper combination of workpiece material, lubrication, and nanoparticles, which are highly efficient and inexpensive for the machining of specific material. For example, a lubrication and nanoparticles used for the machining of hard material can be expensive for the softer materials. The alloy chosen for this research is commonly used in machining application due to its high strength and corrosion resistance. However, little study is observed on investigating the effects of these cutting conditions on Ra along with MRR for this specific aluminum alloy in face milling process. Therefore, this study aims to analyze the impact of dry, MQL, and nanofluid cutting conditions on Ra and MRR. The influence of three effective input variables including Fr, Vs, and Dc has been investigated using Taguchi method.

The rest of this paper is organized as follows. Section 2 explains the experimental procedure for the machining of aluminum specimens with dry, MQL, and nanofluid medium and the Taguchi method used for the design of experiment. Investigated results, analysis using ANOVA, and optimization through contour plots have been presented in Section 3. Finally, conclusions of overall research and recommendations for the future study are discussed in Section 4.

Table 1 Properties of Al6082-T6 [37]

Properties	Value
Density (g/cm^3)	2.7
Hardness (Vickers)	95
Ultimate tensile strength (MPa)	300
Yield strength (MPa)	255
Elongation at break (%)	10
Modulus of elasticity (GPa)	69
Shear strength (MPa)	200
Modulus (GPa)	26

2 Experimental procedure

This section gives a detail about material composition, experimental setup, sample preparation, and response measurements. Aluminum alloy 6082-T6 selected for the machining purpose having mechanical properties and composition is given in Tables 1 and 2, respectively. Optical emission spectrometer is operated to check the chemical composition of workpiece material used. Machining of workpiece material highly depends upon its mechanical properties. Machinability refers to the ease of cutting of metal and allowing the removal of material swiftly. Materials with superior machinability require less cutting power

Table 2 Chemical composition of aluminum alloy (Al-6082)

Si	Fe	Zn	Cr	Mg	Mn	Cu	Al	Others
1.2	0.33	0.05	0.14	0.78	0.5	0.08	Bal	0.15

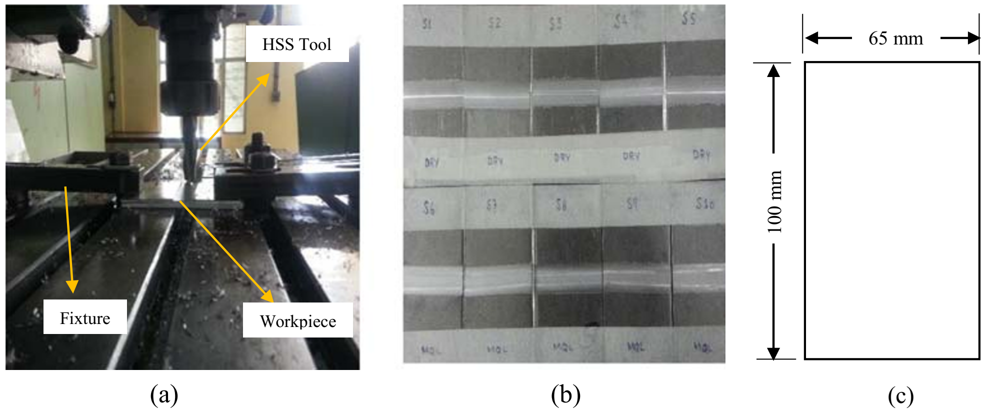

Fig. 1 **a** Face milling process of aluminum specimen, **b** machined specimens, and **c** dimensions of specimen prepared for machining

and time. Machinability of aluminum is considered to be excellent in terms of achieving minimum Ra and maximum MRR. To further improve the machinability of the selected workpiece material, different parameters and cutting conditions have been adopted. From the previous research, it has been observed that Fr, Vs, and Dc are the most effective input parameters for Ra and MRR [38–40]. Therefore, Fr, Vs, and Dc are used as process variables in three different cutting conditions: dry, MQL, and nanofluid. Fr is the linear motion of tool throughout the machining. Vs is the rotational motion of tool, and Dc is controlled by the vertical movement of the tool. Commercial soluble oil is used as lubricant in MQL machining. A system has been developed for the delivery of MQL between the tool and workpiece interface. Air pressure gun attached with a compressor has been employed to throw air-lubricant mist using 5-bar pressure. The oil mist has been produced inside the tank using air pressure. Flow rate of aerosol has been kept constant at 400 ml/h. In nanofluid, Al_2O_3 nanoparticles of size 80 μm mixed with soluble oil in 5% by weight ratio were used with the same flow rate.

Machining process is performed using NC MIKRON WF21C milling machine having maximum Vs of 4000 rpm as shown in Fig. 1a. Workpiece is clamped using fixtures to avoid any vibration and distortion during the machining. To avoid the effect of machine-tool fixture environment on the machining rate and quality, all workpieces are clamped with same type and number of fixtures. Use of proper machine tool fixtures enables experimental process to present the true effects of input parameters and cutting conditions. Cutting tool made of HSS with 16 mm diameter is employed. The specimens prepared for the face milling process along with dimensions are shown in Fig. 1 b and c, respectively. Surface roughness of the specimens was measured through surface roughness tester, shown in Fig. 2.

Fig. 2 Surface roughness measuring apparatus

2.1 Experimental design

Taguchi design is a robust technique used for the optimization of input variables and reduces the process variation. The technique uses signal-to-noise (S/N) ratio as quality characteristic measurement [41]. Using S/N ratios, Taguchi empirically found the two-stage optimization process indeed offers the optimum level combination while keeping mean on target, minimizing the standard deviation [42]. S/N ratio is beneficial in improvement of measurement and improving quality through variability reduction. Properties of S/N can be classified in three categories:

$$\text{Smaller the better property; } S/N = -10\log\frac{1}{n}\left(\sum Y^2\right) \tag{1}$$

$$\text{Nominal the best property; } S/N = 10\log\frac{\overline{Y}}{S_y^2} \tag{2}$$

Table 3 Face milling input variables with levels

Input Variables	Levels		
	Low	Medium	High
Feed rate (mm/min)	500	1000	2000
Spindle speed (rpm)	1000	2000	4000
Depth of cut (mm)	0.25	0.5	1

Table 4 Design matrix with observed responses

Exp. run	Input variables			Response variables								
	Feed rate (mm/min)	Spindle speed (rpm)	Depth of cut (mm)	Surface roughness (µm)						Material removal rate (mm^3/sec)		
				Dry		MQL		Nanofluid		Dry	MQL	Nanofluid
				Mean	Std. dev	Mean	Std. dev	Mean	Std. dev			
1.	500	1000	0.25	1.105	0.0042	0.785	0.0089	0.683	0.00025	30.906	29.606	30.556
2.	500	2000	0.5	0.940	0.00098	0.677	0.00064	0.582	0.00051	75.811	76.931	75.901
3.	500	4000	1	0.658	0.00027	0.480	0.00091	0.403	0.00029	148.620	149.342	148.892
4.	1000	1000	0.5	1.713	0.0016	1.216	0.00022	1.046	0.0054	149.622	147.622	151.523
5.	1000	2000	1	1.542	0.0075	1.141	0.0021	1.016	0.00069	289.774	287.224	290.534
6.	1000	4000	0.25	0.694	0.00051	0.486	0.00062	0.423	0.00024	69.811	69.781	67.764
7.	2000	1000	1	3.381	0.0232	2.468	0.071	2.172	0.039	506.489	508.490	506.015
8.	2000	2000	0.25	2.339	0.0099	1.684	0.0064	1.465	0.0087	163.552	161.622	163.642
9.	2000	4000	0.5	1.520	0.0056	1.064	0.0051	0.936	0.00061	269.244	271.894	269.723

$$\text{Larger the better property; } S/N = 10\log\frac{1}{n}\left(\sum\frac{1}{Y^2}\right) \quad (3)$$

where Y is mean of all the observed values, S_y^2 is variance of y, y is observed data, and n depicts number of observed values. Smaller the better case was employed for Ra and larger the better for MRR. Fr, Vs, and Dc have been specified as input variables due to their remarkable impact on machining properties [43–46]. The input variables along with selected levels are shown in Table 3.

Nine experiments were performed using Taguchi method L_93^4 array for each cutting condition. Experiments were performed at each level of the input variables to measure the response variables included Ra and MRR. Three different readings of the machined surface have been taken for each specimen and their mean value is considered as final reading. Mean and standard deviation of the measured values against each experimental run have been presented in Table 4. MRR is calculated using Eq. 4 [47].

$$MRR = \frac{(W_1 - W_2)}{t \times \rho} \quad (4)$$

Here W_1 is initial weight of a specimen before machining, W_2 is final weight after machining, ρ is density of workpiece material, and t is machining time.

3 Results and discussion

3.1 Graphical representation using signal-to-noise ratio approach

Taguchi's S/N ratio represents the response or quality characteristics, and the largest S/N ratio value is desirable. S/N ratio was used for selecting the best combination of input variables to achieve optimum response. Average values of signal-to-noise ratio for Ra of different variables at their levels are shown in Table 5 and represented in graphical form in Fig. 3. The peak values of S/N ratio of control variables were selected representing the optimum conditions for the Ra. S/N ratio is also used to rank the input parameters on the basis of their

Table 5 Average values of S/N ratios of Ra at different levels

Level	Dry			MQL			Nanofluid		
	Fr	Vs	Dc	Fr	Vs	Dc	Fr	Vs	Dc
1.	1.103	− 5.376	− 1.722	3.9573	− 2.4815	1.2833	5.3020	− 1.2715	2.4930
2.	− 1.785	− 3.533	− 2.591	1.1411	− 0.7594	0.3842	2.3184	0.4179	1.6276
3.	− 7.199	1.028	− 3.568	− 4.3043	4.0349	− 0.8735	− 3.1609	5.3131	0.3388
Delta	8.303	6.404	1.846	8.2616	6.5164	2.1568	8.4629	6.5846	2.1541
Rank	1	2	3	1	2	3	1	2	3

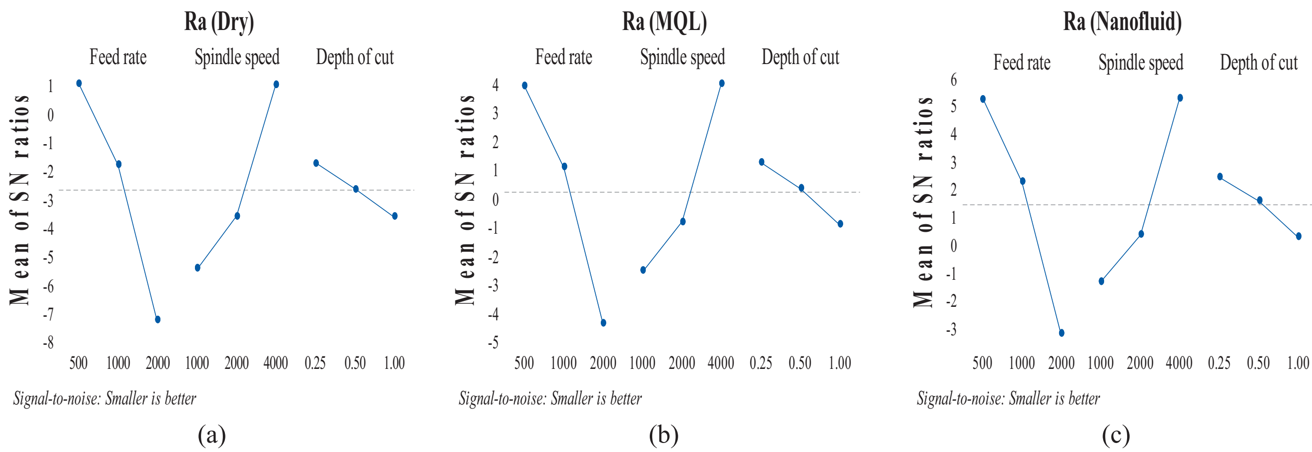

Fig. 3 S/N ratio graph showing the effects of Fr, Vs, and Dc on Ra for **a** dry, **b** MQL, and **c** nanofluid

contribution in Ra. Fr is the highest contributing factor followed by the Vs and Dc. At higher values of Fr and Dc and lower values of Vs, deformed chip cross section and volume and sharp and brittle fractures occur on the machining surface which increases the surface roughness [48, 49]. In dry condition, Ra is found to be minimum at low level of Fr and Dc and high level of Vs. Similar trends are observed for MQL and nanofluid cutting conditions as shown in Fig. 3 b and c, respectively.

Average values of signal to noise ratio for MRR are given in Table 6, and graph for the S/N ratio are presented in Fig. 4. Ranking of input parameters on the basis of their S/N ratio shows that Fr is the most contributing input parameter for MRR, while Dc and Vs are the second and third most contributing input parameters, respectively, and same can be seen in Fig. 4. MRR is maximum at high level of Fr and Dc and mid-level of Vs.

3.2 Analysis of results through analysis of variance

For the modeling of response variables, regression analysis is performed using statistical software Minitab. Analysis of variance (ANOVA) is employed to test the adequacy of the developed models.

Table 6 Average values of S/N ratio of MRR at different levels

Level	DRY			MQL			Nanofluid		
	Fr	Vs	Dc	Fr	Vs	Dc	Fr	Vs	Dc
1	36.95	42.46	36.98	36.88	42.31	36.82	36.92	42.46	36.87
2	43.21	43.70	43.23	43.14	43.69	43.26	43.16	43.72	43.28
3	48.99	42.97	48.92	48.99	43.01	48.92	48.99	42.90	48.93
Delta	12.04	1.24	11.94	12.12	1.37	12.10	12.07	1.25	12.07
Rank	1	3	2	1	3	2	1	3	2

3.2.1 ANOVA for Ra

ANOVA results declared that the effects of input variables, Fr, Vs, and Dc associated with Ra, were significant for dry conditions. Same input variables were obtained significant for MQL and nanofluid cutting. ANOVA results along with adequacy measures R^2, adjusted R^2, and predicted R^2 values are provided in Table 4. The results demonstrate that the regression models are significant having p value less than 0.05. Adequacy measures R^2, R^2 (adjusted), and R^2 (predicted) values for dry, MQL, and nanofluid conditions are close to one, indicating the adequacy of models. For the prediction of Ra, empirical models for dry, MQL, and nanofluid conditions are presented in Eqs. 5, 6, and 7, respectively.

$$\text{Ra (Dry)} = 0.801 + 0.001021 \times \text{Fr}{-}0.000363 \times \text{Vs} + 0.684 \times \text{Dc} \quad (5)$$

$$\text{Ra (MQL)} = 0.561 + 0.000737 \times \text{Fr}{-}0.000267 \times \text{Vs} + 0.540 \times \text{Dc} \quad (6)$$

$$\text{Ra (Nanofluid)} = 0.472 + 0.000653 \times \text{Fr}{-}0.000313 \times \text{Vs} + 0.486 \times \text{Dc} \quad (7)$$

Percentage contribution of each factor in Ra for all cutting conditions extracted from the ANOVA tables has been presented as pie charts in Fig. 5a. Fr is the most contributing factor for Ra with percentage contribution of 60%. Percentage contribution of Vs and Dc are 30% and 7%, respectively.

3.2.2 ANOVA for MRR

The input parameters that significantly influence in MRR include Fr and Dc. Models developed for MRR are significant with p value less than 0.05 as shown in Table 7. Adequacy measures R^2, R^2 (adjusted), and R^2 (predicted) are close to one, showing the adequacy of the models. For the prediction of MRR, empirical models for dry, MQL, and nanofluid are developed and presented in Eqs. 8, 9, and 10, respectively.

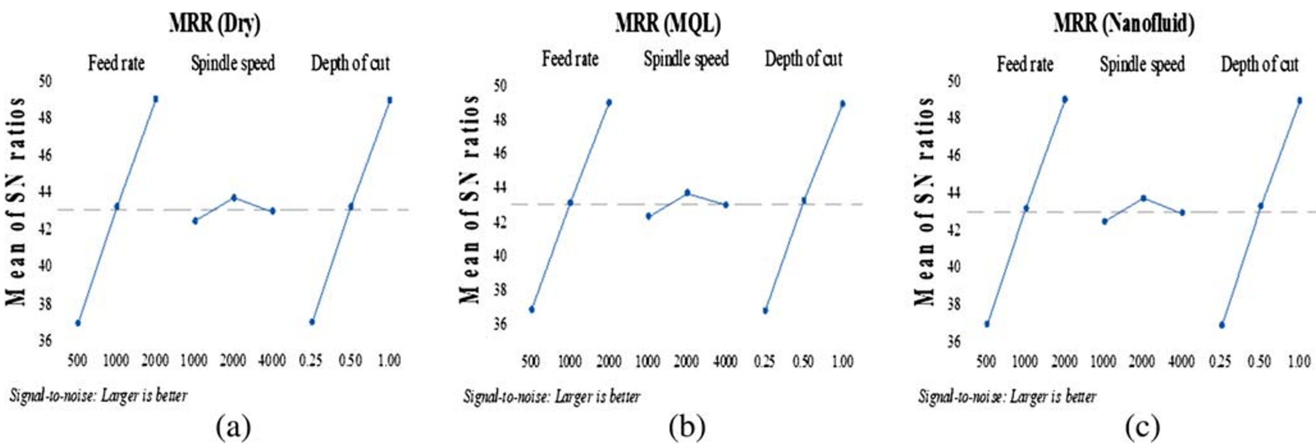

Fig. 4 S/N ratio graph showing the effects of Fr, Vs, and Dc on MRR for **a** dry, **b** MQL, and **c** nanofluid

$$\text{MRR (Dry)} = -116.2 + 0.1508 \times \text{Fr} - 0.0200 \times \text{Vs} + 302.2 \times \text{Dc} \quad (8)$$

$$\text{MRR (MQL)} = -119.3 + 0.1515 \times \text{Fr} - 0.0194 \times \text{Vs} + 303.3 \times \text{Dc} \quad (9)$$

$$\text{MRR (Nanofluid)} = -116.0 + 0.1507 \times \text{Fr} - 0.0203 \times \text{Vs} + 303.3 \times \text{Dc} \quad (10)$$

Pie chart in Fig. 5b showing the percentage contribution of different input variables for MRR has been obtained from the ANOVA table. Fr and Dc are the major contributing factors with percentage contribution of 46% each. Vs has very small contribution in achieving maximum MRR.

3.3 Optimization using contour plots

Contour plots are normally used for the optimization and prediction of the response variables. Optimization of milling process can be considered as multivariate and multi-criteria problems in which the objective is to maximize or minimize the single variable. Here the effects of input variables on Ra and MRR have been analyzed using contour plots. It is apt that the graphs represent the effects of two input variables at the middle level of all the other variables.

3.3.1 Contour plots for Ra

Figure 6a–c represents the effects of Fr and Vs on Ra for dry, MQL, and nanofluid, respectively. By comparing the Ra of dry, MQL, and nanofluid cutting conditioned parts, it is evident that the effect of Fr and Vs on Ra are similar. Ra is more sensitive to Fr as compared with Vs. Moreover, Ra decreases with increasing Vs and decreasing Fr. It is virtuous to state that minimum Ra is achieved in nanofluid cutting condition as compared with dry and MQL.

The effects of input variables Fr and Dc for all cutting conditions are shown in Fig. 7 a to c. The contour plot demonstrates that Ra is affected by Fr significantly, and it is less altered by Dc and same trend has been observed in all cutting conditions. Among three different types of cutting conditions, nanofluid machining yields better results.

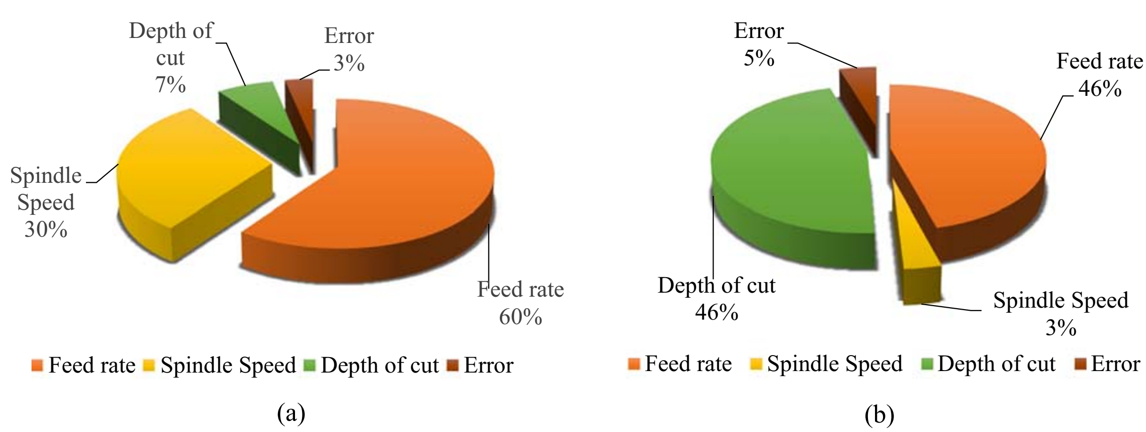

Fig. 5 Pie chart of percentage contributions for **a** Ra and **b** MRR

Table 7 Analysis of variance for Ra and MRR

	Surface Roughness (Dry)					
Source	DF	Adj SS	Adj MS	F-Value	P-Value	
Regression	3	5.904	1.968	50.12	<0.0001	Significant
Fr	1	3.648	3.648	92.90	<0.0001	
Vs	1	1.847	1.847	47.05	0.001	
Dc	1	0.409	0.409	10.42	0.023	
Error	5	0.196	0.039			
Total	8	0.039				
			Model Summary			
R^2	96.78%	R^2 (adj)	94.85%	R^2 (Pred)	85.73%	
	Surface Roughness (MQL)					
Source	DF	Adj SS	Adj MS	F-Value	P-Value	
Regression	3	3.155	1.051	46.76	<0.0001	Significant
Fr	1	1.899	1.899	84.46	<0.0001	
Vs	1	1.001	1.001	44.49	0.001	
Dc	1	0.255	0.255	11.35	0.020	
Error	5	0.112	0.022			
Total	8	3.267				
Model Summary						
R^2	96.56%	R^2 (adj)	94.49%	R^2 (Pred)	84.84%	
	Surface Roughness (Nanofluid)					
Source	DF	Adj SS	Adj MS	F-Value	P-Value	
Regression	3	2.469	0.823	49.67	<0.0001	Significant
Fr	1	1.491	1.491	90.02	<0.0001	
Vs	1	0.770	0.770	46.50	0.001	
Dc	1	0.207	0.207	12.49	0.017	
Error	5	0.082	0.016			
Total	8	2.552				
			Model Summary			
R^2	96.75%	R^2 (adj)	94.81%	R^2 (Pred)	85.76%	

	Material Removal Rate (Dry)					
Source	DF	Adj SS	Adj MS	F-Value	P-Value	
Regression	3	165017	55006	33.48	0.001	Significant
Fr	1	79545	79545	48.41	0.001	
Vs	1	5584	5584	3.40	0.125	
Dc	1	79888	79888	48.62	0.001	
Error	5	8216	1643			
Total	8	173233				
			Model Summary			
	R^2	95.26%	R^2(adj)	92.41%	R^2(pred)	78.32%
	Material Removal Rate (MQL)					
Source	DF	Adj SS	Adj MS	F-Value	P-Value	
Regression	3	166115	55372	31.82	0.001	Significant
Fr	1	80352	80352	46.18	0.001	
Vs	1	5255	5255	3.02	0.143	
Dc	1	80508	80508	46.27	0.001	
Error	5	8699	1740			
Total	8	174815				
Model Summary						
	R^2	95.02%	R^2(adj)	92.04%	R^2(pred)	77.29%
	Material Removal Rate (Nanofluid)					
Source	DF	Adj SS	Adj MS	F-Value	P-Value	
Regression	3	165647	55216	34.83	0.001	Significant
Fr	1	79536	79536	50.17	0.001	
Vs	1	5742	5742	3.62	0.115	
Dc	1	80369	80369	50.70	0.001	
Error	5	7926	1585			
Total	8					
			Model Summary			
R^2	95.43%	R^2 (Adj)	92.69%	R^2 (Pred)	79.14%	

While distinguishing the influence of Vs and Dc on Ra under dry, MQL, and nanofluid cutting conditions, identical trends have been observed (Fig. 8 a to c). Ra decreases with increasing Vs and decreasing Dc. Among different cutting conditions, nanofluid produces the improved surface quality.

3.3.2 Contour plots for MRR

Based on the previous discussions, Fr and Dc are significant factors for MRR. Therefore, it is no need to consider the Vs in MRR optimization. From Fig. 9 a to c, it is cleared that MRR is maximum at high level of Fr and Dc. And different cutting conditions have no effect on MRR.

3.4 Comparison of cutting conditions (dry, MQL, and nanofluid)

It is observed that MQL is better than dry cutting and nanofluid lubrication is better than MQL cutting for Ra. Observed responses of dry, MQL, and nanofluid conditions are compared in Fig. 10. The figure has been drawn from the design matrix given in Table 3. From the Fig. 10, it is evident that shifting from dry to MQL cutting, Ra improve from 26%~30% and further switching from MQL to nanofluid

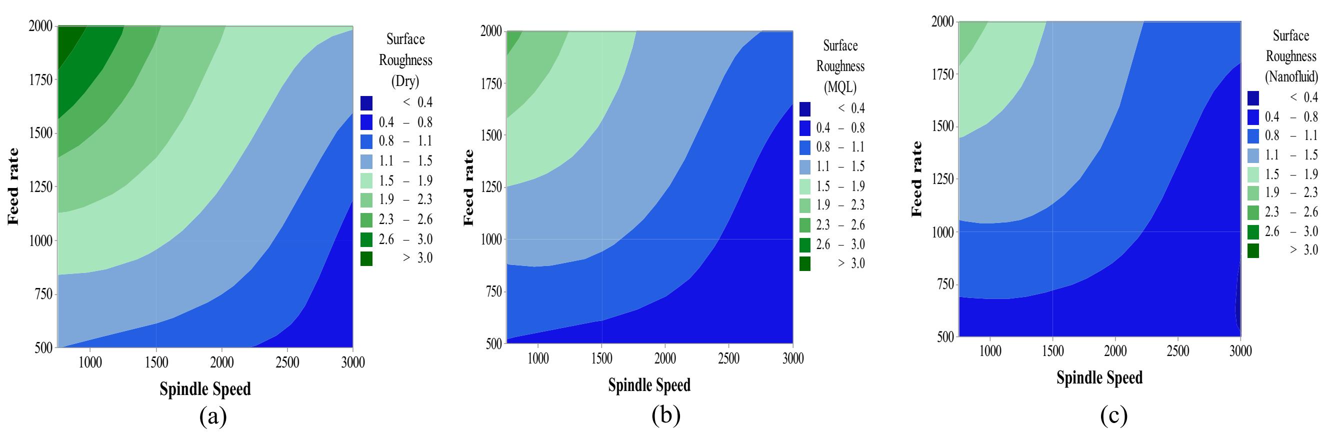

Fig. 6 Contour plots of Ra vs Fr and Vs **a** dry, **b** MQL, and **c** nanofluid

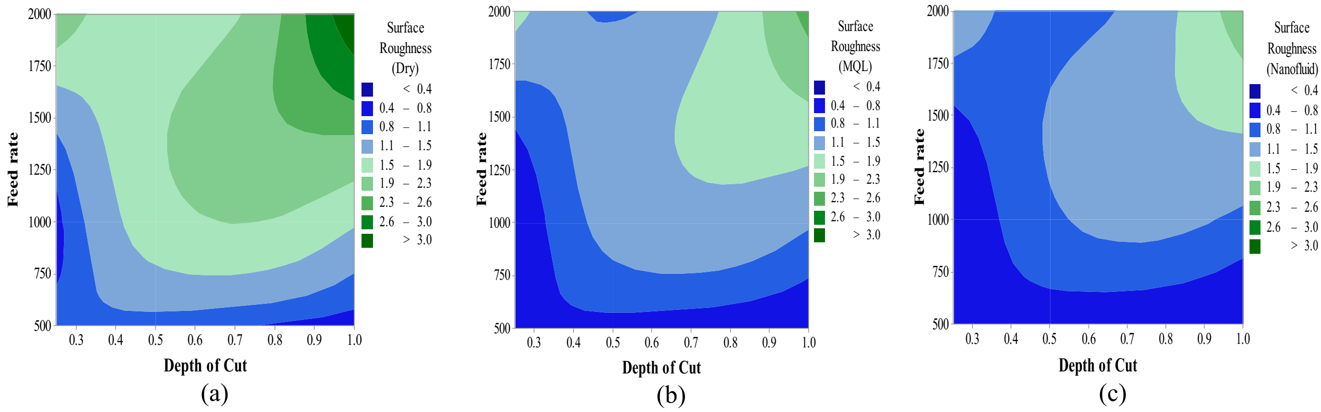

Fig. 7 Contour plots for Ra vs Dc and Fr **a** dry, **b** MQL, and **c** nanofluid

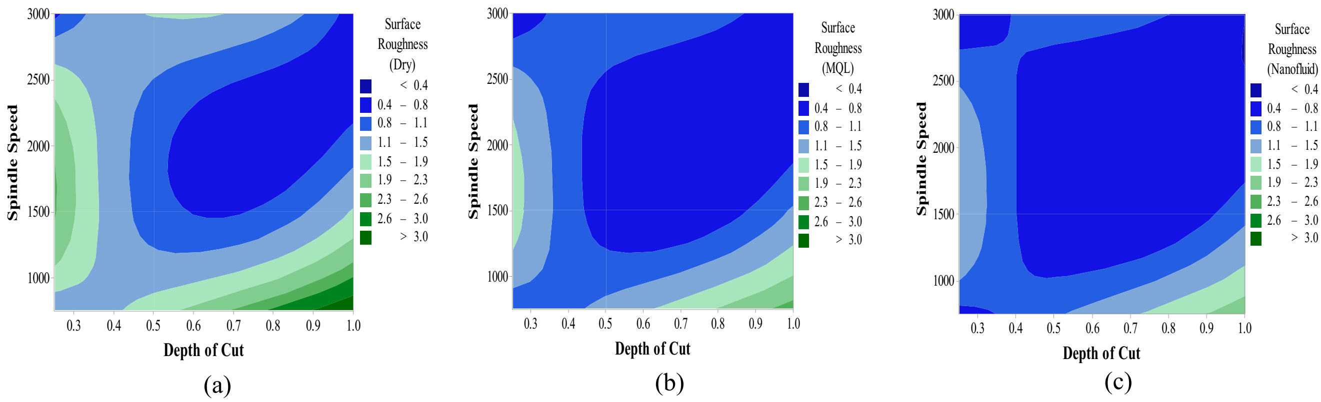

Fig. 8 Contour plots of Ra vs Dc and Vs **a** dry, **b** MQL, and **c** nanofluid

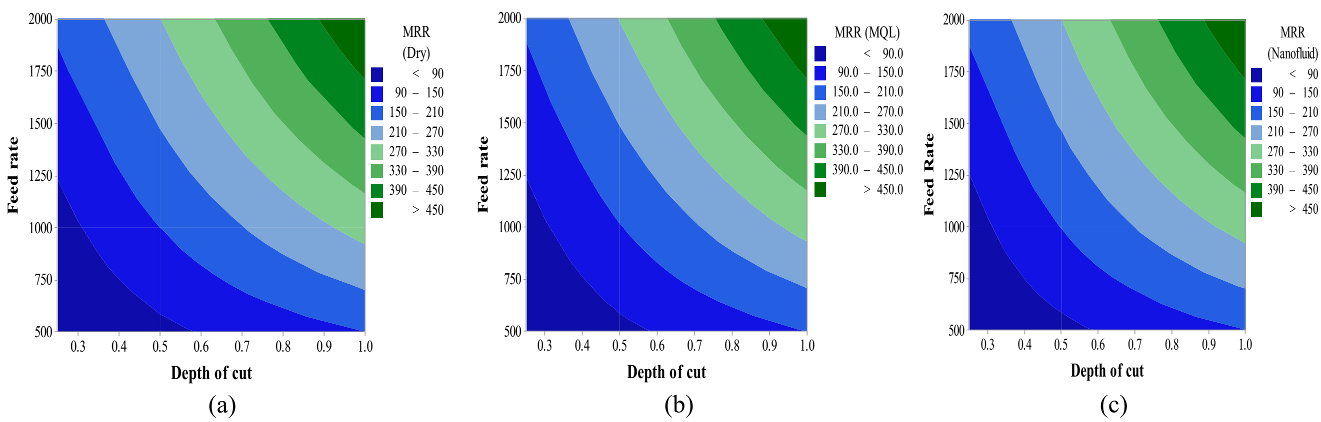

Fig. 9 Contour plots of MRR vs D*c* and Fr **a** dry, **b** MQL, and **c** nanofluid

Fig. 10 Percentage improvement results of Ra

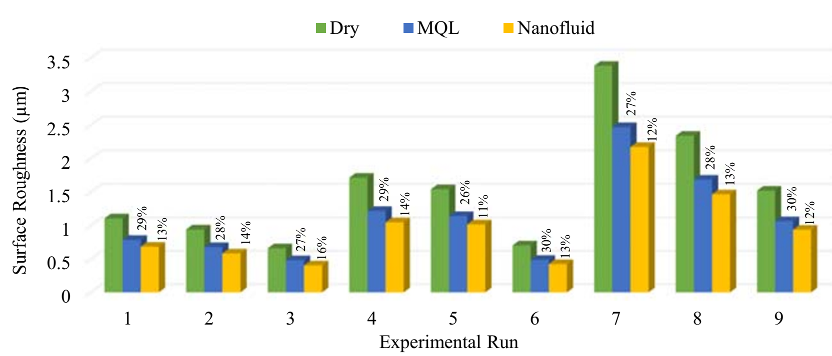

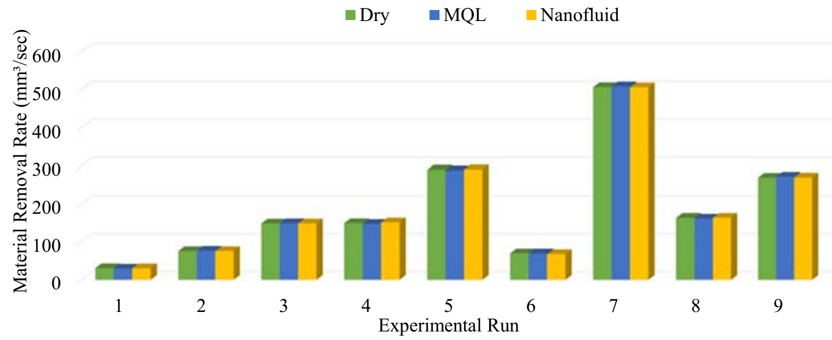

Fig. 11 Percentage improvement results of MRR

cutting, 13%~16% improvement has been observed. In MQL, lubricant penetrates in the machining zone between tool and workpiece with air pressure in a very effective way which reduces the surface roughness [50]. Moreover, in nanofluid, the particles present in the lubricant possess filling and polishing effect and rolled at tool-workpiece interface which reduces the Ra and frictional co-efficient [51, 52]. From Fig. 11, it can be clearly seen that variation in cutting conditions has no effect on MRR, while negligible variation has been observed which can be due to the equipment and human error.

4 Conclusion

The focus of this research is to analyze the effects of dry, MQL, and nanofluid cutting conditions in face milling process for Al-6082 alloy. The effects of Fr, Vs, and Dc on Ra and MRR are analyzed for dry, MQL, and nanofluid cutting conditions using Taguchi method.

- The experimental results reveal that for Ra, (1) Fr is most significant input variables with percentage contribution of 60%; (2) Vs is significant with percentage contribution of 30%; and (3) Dc is less significant as compared with feed rate and Vs with percentage contribution of 7% for dry, MQL, and nanofluid cutting conditions.
- For material removal rate, Fr and Dc are significant factors with percentage contribution of 46% each for all cutting conditions, while Vs is not as significant as Fr and Dc.
- Comparative analysis for Ra shows that the 26~30% improvement will be achieved when shifted from dry to MQL and 13~16% improvement will be obtained when further move to nanofluid cutting condition.
- Negligible effect of cutting conditions (dry, MQL, and nanofluid) is observed for material removal rate.
- Other machining conditions including machine tool fixture environment are kept constant for all experiments to avoid their influence on surface roughness.

This research verified that the proposed nanofluid cutting condition for face milling process could be used by the practitioners to improve the quality of machined parts. Furthermore, the contour plots and developed empirical models for Ra and MRR will aid practitioners to select the optimum level of input variables for the desired Ra and MRR.

As aluminum is a softer material, therefore, it is necessary to use some soft nanoparticles in lubricant to keep surface roughness at its minimum level. Therefore, future study can be conducted on the comparative analysis of the performance of metallic and non-metallic or some soft nanoparticles in the lubricant. If non-metallic nanoparticles yield low surface roughness, then further studies will be conducted to optimize the particle's size and concentration with respect to workpiece materials. The lowest surface roughness achieved in case of soft nanoparticles will eliminate the post-processing of workpiece material. Elimination of single process on industrial scale may reduce the consumption of resources. Moreover, the combination of such nanoparticles and some environmental friendly lubricants can be used to make the process healthy on industrial scale.

References

1. Benardos P, Vosniakos GC (2002) Prediction of surface roughness in CNC face milling using neural networks and Taguchi's design of experiments. Robot Comput Integr Manuf 18(5-6):343–354
2. Lee T, Lin Y (2000) A 3D predictive cutting-force model for end milling of parts having sculptured surfaces. Int J Adv Manuf Technol 16(11):773–783
3. Korkut I, Donertas M (2007) The influence of feed rate and cutting speed on the cutting forces, surface roughness and tool–chip contact length during face milling. Mater Des 28(1):308–312
4. Baek DK, Ko TJ, Kim HS (2001) Optimization of feedrate in a face milling operation using a surface roughness model. Int J Mach Tools Manuf 41(3):451–462
5. Fratila D, Caizar C (2011) Application of Taguchi method to selection of optimal lubrication and cutting conditions in face milling of AlMg3. J Clean Prod 19(6-7):640–645

6. Ozcelik B, Oktem H, Kurtaran H (2005) Optimum surface roughness in end milling Inconel 718 by coupling neural network model and genetic algorithm. Int J Adv Manuf Technol 27(3-4):234–241
7. Bhavsar SN, Aravindan S, Rao PV (2015) Investigating material removal rate and surface roughness using multi-objective optimization for focused ion beam (FIB) micro-milling of cemented carbide. Precis Eng 40:131–138
8. Parashar V, Purohit R (2017) Investigation of the effects of the machining parameters on material removal rate using Taguchi method in EndMilling of Steel Grade EN19. Mater Today Proc 4(2):336–341
9. Chen SH, Kuo CP, Ling CC (2007) On tool-chip interface stress distributions ploughing force and size effect in machining inconel-718 and AISI4340. J Chin Inst Eng 30(2):211–218
10. Yan J, Li L (2013) Multi-objective optimization of milling parameters – the trade-offs between energy, production rate and cutting quality. J Clean Prod 52:462–471
11. Kuram E, Ozcelik B, Bayramoglu M, Demirbas E, Simsek BT (2013) Optimization of cutting fluids and cutting parameters during end milling by using D-optimal design of experiments. J Clean Prod 42:159–166
12. Sayuti M, Sarhan AAD, Tanaka T, Hamdi M, Saito Y (2013) Cutting force reduction and surface quality improvement in machining of aerospace duralumin AL-2017-T4 using carbon onion nanolubrication system. Int J Adv Manuf Technol 65(9-12):1493–1500
13. Wakabayashi T, Suda S (2008) Environmentally friendly machining of aluminum using minimal quantity lubrication system. In: Manufacturing Systems and Technologies for the New Frontier. Springer, pp 377–380
14. Klocke F, Eisenblätter G (1997) Dry cutting. CIRP Ann 46(2):519–526
15. Tosun N, Huseyinoglu M (2010) Effect of MQL on surface roughness in milling of AA7075-T6. Mater Manuf Process 25(8):793–798
16. Zhang S, Li J, Wang Y (2012) Tool life and cutting forces in end milling Inconel 718 under dry and minimum quantity cooling lubrication cutting conditions. J Clean Prod 32:81–87
17. Li K-M, Chou S-Y (2010) Experimental evaluation of minimum quantity lubrication in near micro-milling. J Mater Process Technol 210(15):2163–2170
18. Liao Y, Lin H, Chen Y (2007) Feasibility study of the minimum quantity lubrication in high-speed end milling of NAK80 hardened steel by coated carbide tool. Int J Mach Tools Manuf 47(11):1667–1676
19. Liao Y, Lin H (2007) Mechanism of minimum quantity lubrication in high-speed milling of hardened steel. Int J Mach Tools Manuf 47(11):1660–1666
20. Da Silva R et al (2011) Tool wear analysis in milling of medium carbon steel with coated cemented carbide inserts using different machining lubrication/cooling systems. Wear 271(9-10):2459–2465
21. Hadi M, Atefi R (2015) Effect of minimum quantity lubrication with gamma-Al 2 O 3 nanoparticles on surface roughness in milling AISI D3 steel. Indian J Sci Technol 8(S3):130–135
22. Rapoport L, Leshchinsky V, Lvovsky M, Nepomnyashchy O, Volovik Y, Tenne R (2002) Mechanism of friction of fullerenes. Ind Lubr Tribol 54(4):171–176
23. Zhang B-S, Xu BS, Xu Y, Gao F, Shi PJ, Wu YX (2011) Cu nanoparticles effect on the tribological properties of hydrosilicate powders as lubricant additive for steel–steel contacts. Tribol Int 44(7-8):878–886
24. Sharma AK, Tiwari AK, Dixit AR (2015) Improved machining performance with nanoparticle enriched cutting fluids under minimum quantity lubrication (MQL) technique: a review. Mater Today Proc 2(4-5):3545–3551
25. Rahmati B, Sarhan AA, Sayuti M (2014) Morphology of surface generated by end milling AL6061-T6 using molybdenum disulfide (MoS2) nanolubrication in end milling machining. J Clean Prod 66:685–691
26. Raza MH et al (2020) Investigating the effects of gating design on mechanical properties of aluminum alloy in sand casting process. J King Saud Univ Eng Sci
27. Tahir W, Jahanzaib M, Ahmad W, Hussain S (2019) Surface morphology evaluation of hardened HSLA steel using cryogenic-treated brass wire in WEDM process. Int J Adv Manuf Technol 104(9):4445–4455
28. Tsao C (2009) Grey–Taguchi method to optimize the milling parameters of aluminum alloy. Int J Adv Manuf Technol 40(1-2):41–48
29. Ali MA et al (2020) Mechanical characterization of aged AA2026-AA2026 overcast joints fabricated by squeeze casting. Int J Adv Manuf Technol
30. Raza MH, Sajid M, Wasim A, Hussain S, Jahanzaib M (2019) Modeling of the mechanical properties of directionally solidified Al-4.3% Cu alloy using response surface methodology. Int J Adv Manuf Technol 103(9):3913–3925
31. Alharthi NH, Bingol S, Abbas AT, Ragab AE, el-Danaf EA, Alharbi HF (2017) Optimizing cutting conditions and prediction of surface roughness in face milling of AZ61 using regression analysis and artificial neural network. Adv Mater Sci Eng 2017:1–8
32. Akhtar MU, Raza MH, Shafiq M (2018) Role of batch size in scheduling optimization of flexible manufacturing system using genetic algorithm. J Ind Eng Int:1–12
33. Montgomery DC (2017) Design and analysis of experiments. Wiley
34. Sofuoğlu MA, Çakır FH, Kuşhan MC, Orak S (2019) Optimization of different non-traditional turning processes using soft computing methods. Soft Comput 23(13):5213–5231
35. Gürgen S, Çakır FH, Sofuoğlu MA, Orak S, Kuşhan MC, Li H (2019) Multi-criteria decision-making analysis of different non-traditional machining operations of Ti6Al4V. Soft Comput 23(13):5259–5272
36. Sofuoğlu MA, Arapoğlu RA, Orak S (2017) Multi objective optimization of turning operation using hybrid decision making analysis. Anadolu Univ Sci Technol A Appl Sci Eng 18(3)
37. Kartal F, Yerlikaya Z, Gökkaya H (2017) Effects of machining parameters on surface roughness and macro surface characteristics when the machining of Al-6082 T6 alloy using AWJT. Measurement 95:216–222
38. Kumar S, Saravanan I, Patnaik L (2020) Optimization of surface roughness and material removal rate in milling of AISI 1005 carbon steel using Taguchi approach. Mater Today Proc 22:654–658
39. Nguyen T-T (2019) Prediction and optimization of machining energy, surface roughness, and production rate in SKD61 milling. Measurement 136:525–544
40. Kulkarni HB et al (2020) Investigations on effect of nanofluid based minimum quantity lubrication technique for surface milling of Al7075-T6 aerospace alloy. Mater Today Proc 27:251–256
41. Park S (1996) Robust design and analysis for quality engineering. Boom Koninklijke Uitgevers
42. Taguchi G, Phadke MS (1989) Quality engineering through design optimization. In: Quality control, robust design, and the Taguchi Method. Springer, pp 77–96
43. Abouelatta O, Madl J (2001) Surface roughness prediction based on cutting parameters and tool vibrations in turning operations. J Mater Process Technol 118(1-3):269–277
44. Özel T, Hsu T-K, Zeren E (2005) Effects of cutting edge geometry, workpiece hardness, feed rate and cutting speed on surface roughness and forces in finish turning of hardened AISI H13 steel. Int J Adv Manuf Technol 25(3-4):262–269

45. Suresh P, Rao PV, Deshmukh S (2002) A genetic algorithmic approach for optimization of surface roughness prediction model. Int J Mach Tools Manuf 42(6):675–680
46. Suresh Kumar Reddy N (2005) Venkateswara Rao, A genetic algorithmic approach for optimization of surface roughness prediction model in dry milling. Mach Sci Technol 9(1):63–84
47. Raza MH, Wasim A, Ali MA, Hussain S, Jahanzaib M (2018) Investigating the effects of different electrodes on Al6061-SiC-7.5 wt% during electric discharge machining. Int J Adv Manuf Technol 99(9-12):3017–3034
48. Cheng K (2008) Machining dynamics: fundamentals, applications and practices. Springer Science & Business Media
49. Altintas Y, Ber A (2001) Manufacturing automation: metal cutting mechanics, machine tool vibrations, and CNC design. Appl Mech Rev 54(5):B84–B84
50. Okafor AC, Nwoguh TO (2020) Comparative evaluation of soybean oil–based MQL flow rates and emulsion flood cooling strategy in high-speed face milling of Inconel 718. Int J Adv Manuf Technol 107(9):3779–3793
51. Liu G, Li X, Qin B, Xing D, Guo Y, Fan R (2004) Investigation of the mending effect and mechanism of copper nano-particles on a tribologically stressed surface. Tribol Lett 17(4):961–966
52. Peng DX, Kang Y, Hwang RM, Shyr SS, Chang YP (2009) Tribological properties of diamond and SiO2 nanoparticles added in paraffin. Tribol Int 42(6):911–917